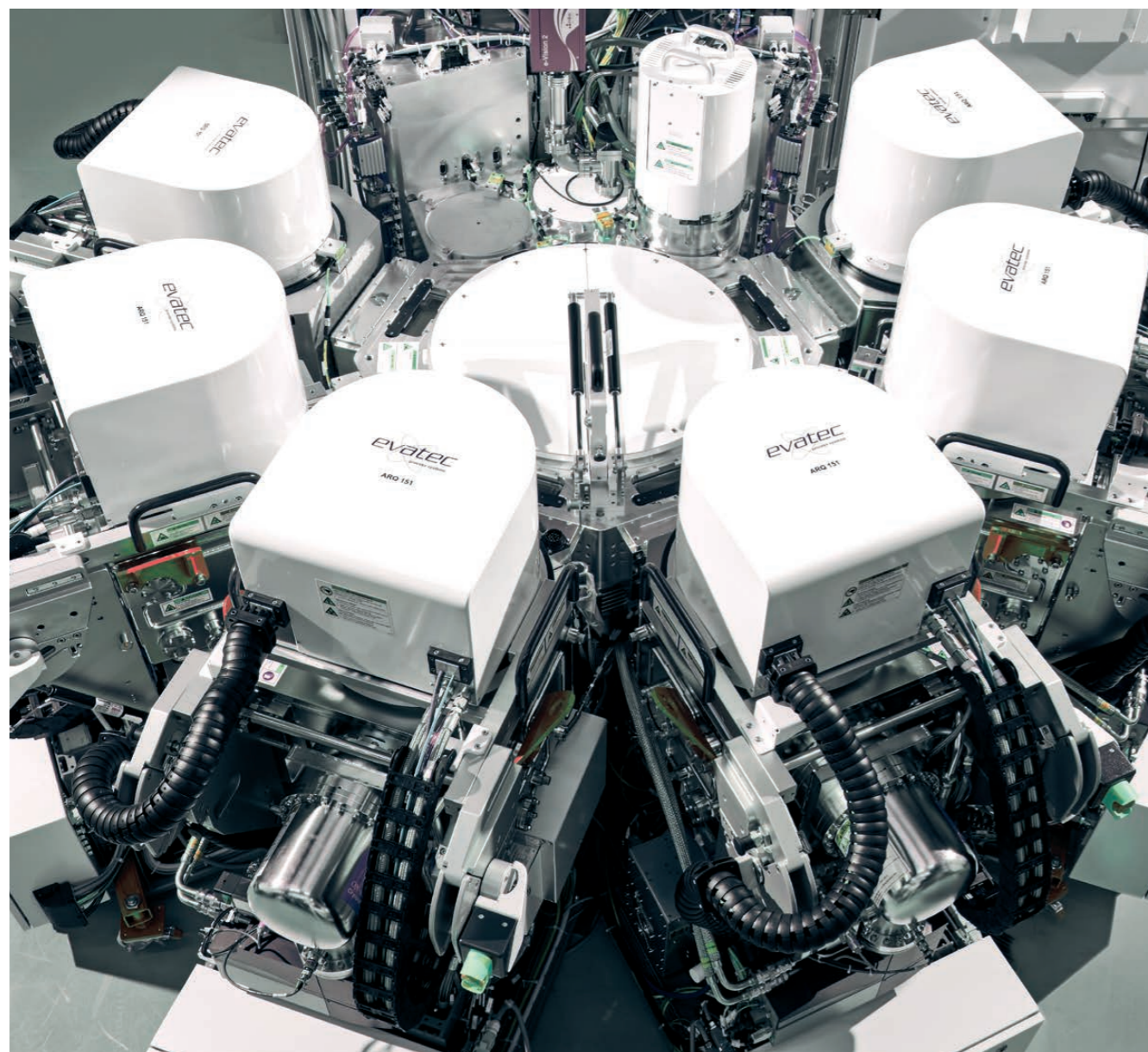


MEETING THE CHALLENGES FOR NEW BAW PROCESSES – VERY HOT CHUCK SOLUTIONS

Evatec's Process Engineering Manager **Martin Kratzer** (corresponding author) and **Dr. Xiang Yao** talk about the technology solutions needed to achieve the deposition processes controlling film crystallinity, stress and thickness uniformity for the thinner films required on 200mm wafers in the RF-BAW filter market.



The RF Filter market remains buoyant

5G wireless technology is driving huge changes in the telecommunication world with transformation to 5G mobile networks creating enormous opportunities for 5G RF filtering technology. According to statistics from Yole, the overall demand for RF filter units has increased consistently by 8% each year for the last 7 years. In particular, we see a sharp expansion for the RF bulk acoustic wave (BAW) filter market, with ongoing shift from surface acoustic wave (SAW) to bulk acoustic wave due to its superior performance at high frequencies as the BAW filter manufacturing process becomes mature and its cost of production goes down. Currently most of the leading players in the BAW market are American based companies, amongst which Evatec's CLUSTERLINE® system has proven itself to be the system of choice for BAW manufacturing.

Challenges in BAW technology

The key component of a typical RF BAW filter has a very simple structure. It contains a piezo layer which is sandwiched in-between top and bottom electrode layers. Depending what is underneath the sandwich structure, it is classified as Film Bulk Acoustic Resonator (FBAR), where an air cavity is under the BAW structure, or Solidly Mounted Resonator (SMR), where an acoustic reflector is under the BAW structure. The material of choice is Al1-xScxN, where we utilize its piezoelectric property along the c-axis of its Wurtzite crystal lattice (d33). The choice of electrode material varies, according to considerations for resistivity, acoustic density, and how well the Wurtzite Al1-xScxN lattice grows on top.

The Figure of Merit (FOM) of a BAW resonator is usually defined as the product of the effective electromechanical coupling coefficient k_{eff}^2 and the quality factor Q . The k_{eff}^2 is measure of how efficiently the energy is transformed between the mechanical and electrical forms in the resonator and is a consequence of both

the piezoelectric coupling coefficient (kt^2) of the piezo-layer and the resonator design, while Q is a measure of energy loss in the resonator. In terms of the RF filtering application, k_{eff}^2 determines the bandwidth of the bandpass filter and Q determines the insertion loss and sharpness of rejection. Development in BAW technology always tends towards higher frequency, broader bandwidth with better power handling performance imposing several challenges for BAW development. Considering the requirements on the Al1-xScxN based piezo-layer, this means a thinner layer structure, as the resonant frequency is inversely proportional to the layer thickness, larger kt^2 for wider bandwidth, and better Q factor for loss reduction and power handling. The coupling coefficient kt^2 of Al1-xScxN layer is a function of its piezoelectric coefficient d_{33} , which is related to the Sc doping level and the piezo-layer stress, as shown in Figure 2a and 2d. The high kt^2 would demand a high level of Sc doping and tensile layer stress. To improve the quality factor, we need to consider the crystallinity of the overall layer structure as well as the electrode design and conductivity.

Nevertheless, the new challenges imposed by the demand for higher frequency, wider bandwidth and better power handling actually put constraints on each other. To utilize the piezoelectric coefficient along the c-axis (d_{33}) of the Al1-xScxN Wurtzite lattice for filtering, a preferential grain orientation, the c-axis $\langle 0002 \rangle$ perpendicular to the film surface, is required for the piezo-layer. A measure of how well the Al1-xScxN grains are aligned is the rocking curve (RC) of the $\langle 0002 \rangle$ peak in the X-ray diffractometry. Generally speaking, a narrower RC FWHM (full width at half maximum) results in a higher kt^2 and Q factor. However, reducing the film thickness usually leads to broader RC FWHM (Figure 2b). Additionally, thinner films tend to show more compressive stress (Figure 2c) due to the lowered wafer temperature during deposition. This again deteriorates the performance of thin films for high frequency

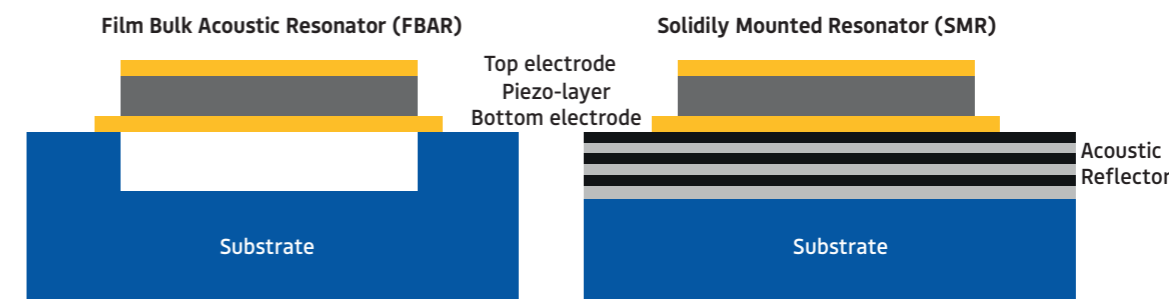


Figure 1:
Comparison of
FBAR and SMR
technologies

applications. Sc doping in AlN would enhance the piezoelectric coefficient of the material, thus increasing the k_t^2 of the piezo-layer in principle. However, when the $Al_{1-x}Sc_xN$ films are doped with high Sc concentrations, the films are usually more compressive in stress and we also face difficulties to align the grains with c-axis orientation out-of-plane. Especially when Sc doping level is high, abnormally orientated grains (AOGs) form through the whole film thickness and roughen the film surface. These are grains with unwanted orientations which worsen the k_t^2 and Q factor of the film. These all cancel the benefit of high Sc doping. On the other hand, if we want to increase the film stress for better k_t^2 , we usually end up with more AOGs. To sum up, when we deposit $Al_{1-x}Sc_xN$ with low thickness and high Sc concentration, we face problems with compressive stress, broader RC FWHM, and more AOGs. So, is there a way that would allow us to overcome those unwanted effects? A very simple

solution is to increase the deposition temperature, which would improve both the film stress and crystallinity, and that brings us to the focus of this article.

For high frequency filtering applications, very thin layer of highly Sc-doped $Al_{1-x}Sc_xN$ films are usually chosen as the piezo-layer. This puts much tighter requirements on the film thickness and stress uniformity. The correlation between k_t^2 and film stress depends on the Sc doping level: the higher the Sc doping, the stronger the correlation. As shown in Figure 2d, for 30% Sc doped $Al_{1-x}Sc_xN$ film, the k_t^2 changes by 1% per 100 MPa, which is huge in terms of band width at high frequencies for the filter device. Therefore, much narrower stress variation across wafer is needed to guarantee the production yield. Evatec has proven expertise in this process optimization and has already demonstrated an optimized sputter source and process kit.

Managing stress and thickness uniformity in production

Currently at Evatec, we adopt two approaches to meet the increasing demand for stress and thickness uniformity. The first approach is based on the already optimized CLUSTERLINE® 200 module with an upgrade of sputter source from ARQ151 DC to ARQ 151 RFDC. We call this upgrade 'High Performance Package' (HPP) where we switch from DC pulsed sputtering to DC+RF sputtering. This offers us additional knobs for very fine optimization of $Al_{1-x}Sc_xN$ film stress. The HPP package offers dramatic improvement in terms of stress range. We can successfully bring down the stress range below 100 MPa for $Al_{1-x}Sc_xN$ film. One example is illustrated for a 20% Sc doped $Al_{1-x}Sc_xN$ film in Figure 3a. In the second approach illustrated in Figure 3b, we show how we can make still further improvements by modifying the DC sputter source usually used for a CLUSTERLINE® 300

module and installing it on a CLUSTERLINE® 200 module with an optimized process kit. Benefited from the large target size, we can achieve excellent thickness uniformity and stress range. The example in Figure 3b shows excellent uniformities below 0.25% and stress range of 100 MPa for 1um AlN film. It has to be noted that all the measurements in Figure 3 were done with 5 mm edge exclusion. The FSM stress measurements were done with 4 lines across the wafer center.

Very Hot Chuck Solutions

The modular design of CLUSTERLINE® platforms offers the flexibility to combine different sputter sources, process kits and chuck types to target the best film performance. With this advantage, we can easily incorporate Very Hot Chuck (VHC) solutions into the

➤➤➤➤➤

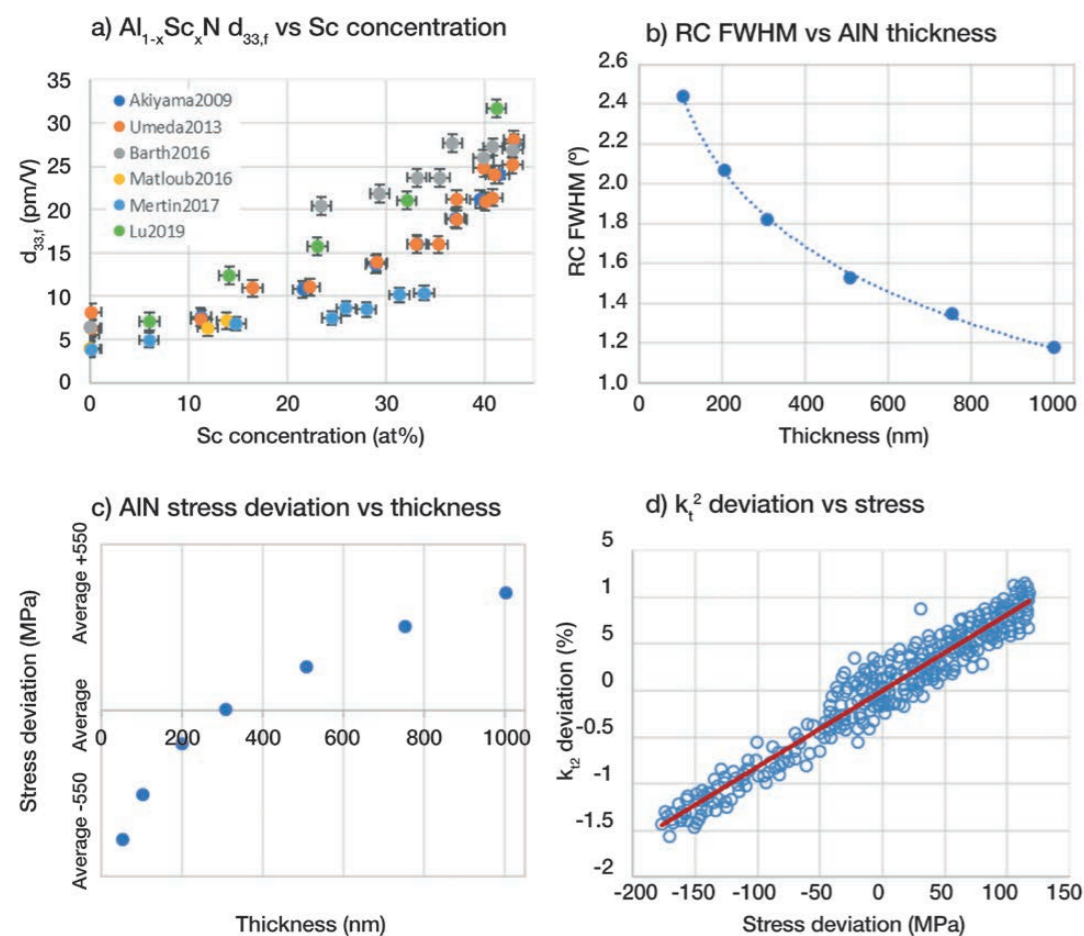


Figure 2: a) $d_{33,f}$ of $Al_{1-x}Sc_xN$ vs Sc concentration, data are collected from Akiyama et al. [1], Umeda et al. [2], Barth et al. [3], Matloub et al. [4], Mertin et al. [5] and Lu [6]. Error bars indicate only the errors from data collection, not the original data error; b) RC FWHM vs AIN thickness; c) AIN stress deviation vs thickness; d) k_t^2 deviation of $Al_{0.7}Sc_{0.3}N$ film vs stress.

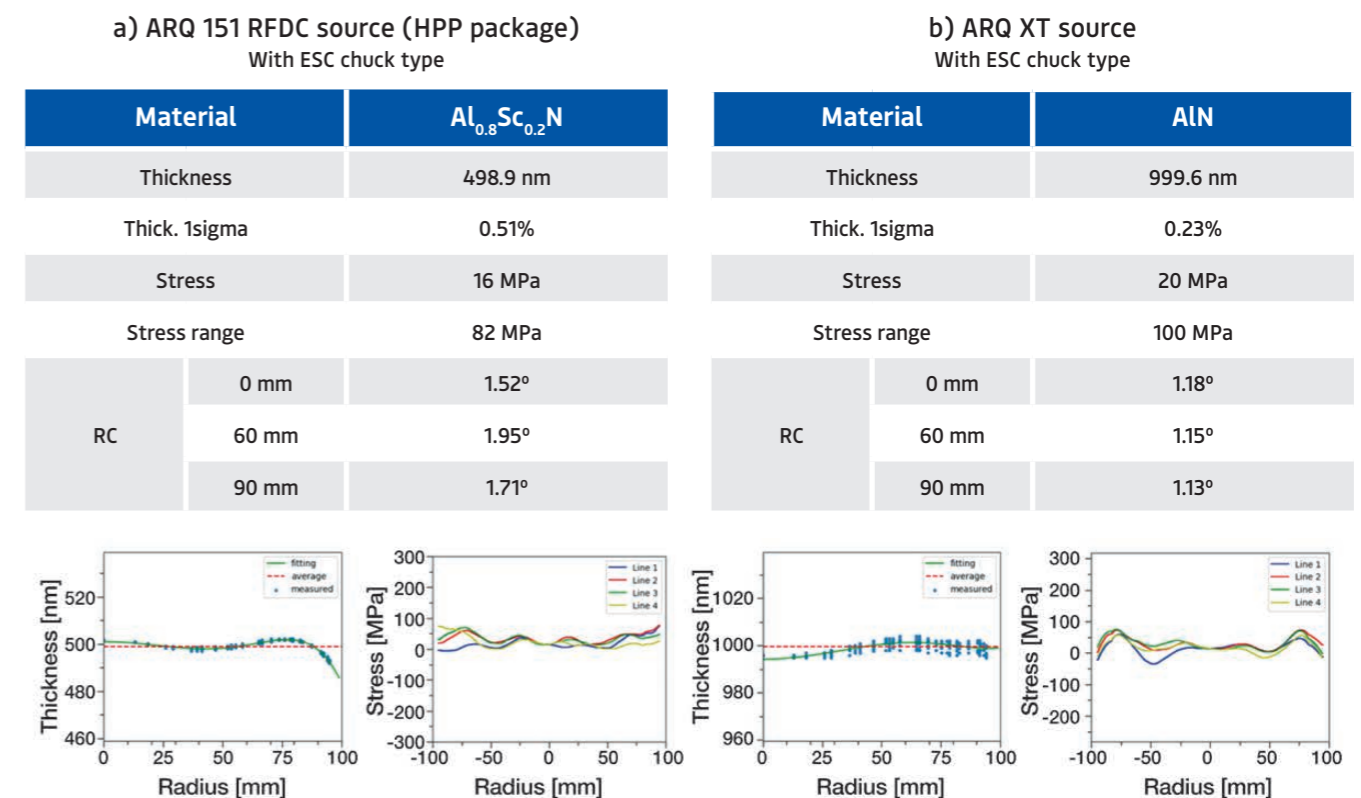


Figure 3: a) Benchmark film performance for $Al_{0.8}Sc_{0.2}N$ film deposition with ARQ151 HPP package; b) Benchmark film performance for AlN film deposition with ARQ-XT source. It has to be noted that the edge exclusion is 5mm for all measurements. FSM measurements were done with 4 lines across the wafer center.

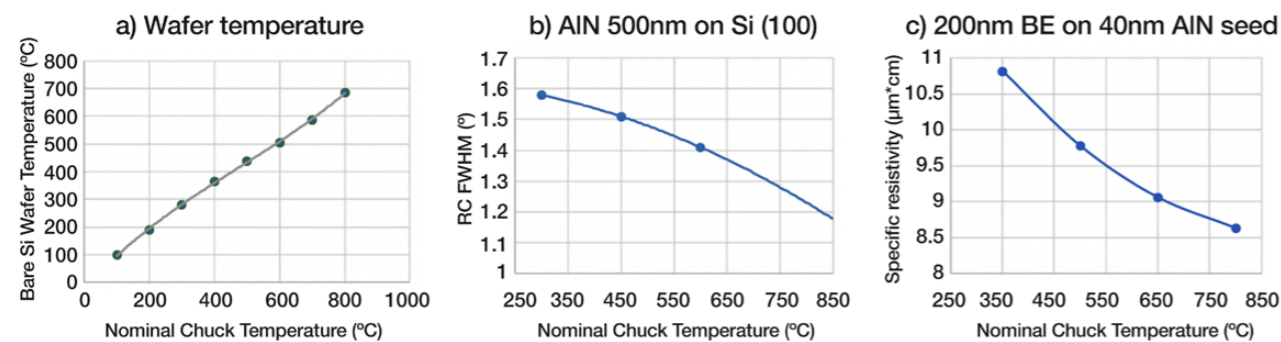


Figure 4: a) wafer temperature measured by thermal couple array wafer at different nominal chuck temperatures of the VHC; b) RC FWHM of AlN 500 nm film at different nominal chuck temperatures of the VHC; c) specific resistivity of a 200 nm bottom electrode (BE) layer at different nominal chuck temperatures of the VHC.

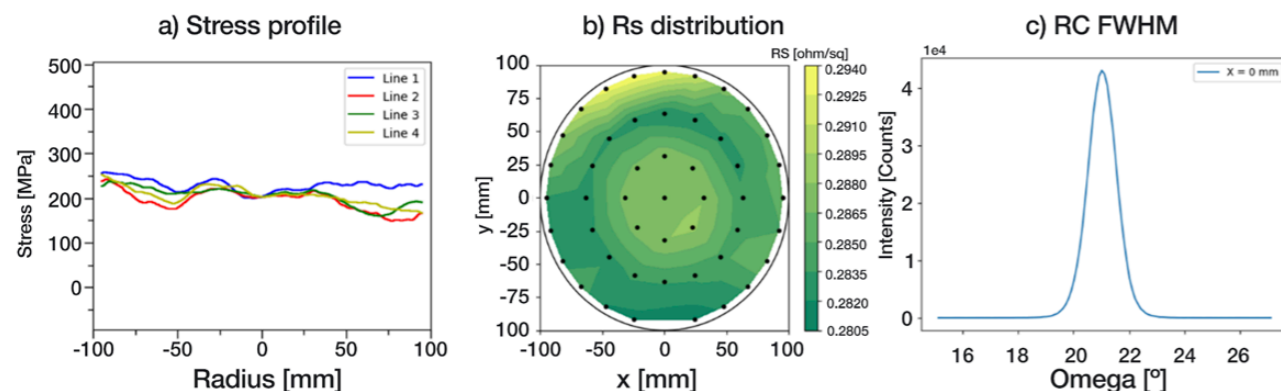


Figure 5: Film performance of one type of bottom electrode (BE) deposited at 800°C by the VHC. a) stress profile across wafer of the bottom electrode with seed layer; b) Rs distribution across wafer; c) RC FWHM at the wafer center.

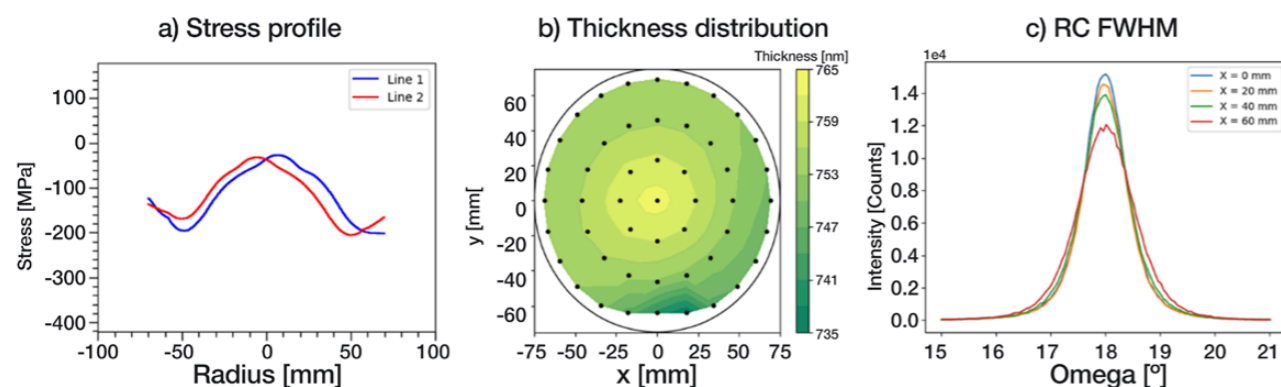


Figure 6: Preliminary results of AlN deposition by VHC at 600°C. a) stress profile across wafer; b) thickness distribution across wafer; c) AlN (0002) RC FWHM at different radial positions.

sputter module with the optimized sputter source and process kits discussed above. The VHC has the capability for temperatures to 800°C. Figure 4a shows wafer temperature measured by thermal couple varying chuck temperatures. With chuck temperature heated up to 800°C, the wafer temperature reaches 700°C offering us a much wider range of temperature for deposition. Preliminary results already show the benefit of high temperature deposition. For example, for deposition of AlN on a Si wafer (Figure 4b), we see decreasing RC FWHM with increasing chuck temperature. Similarly, for bottom electrode (BE) layer deposition, the specific resistivity decreases with increasing chuck temperature (Figure 4c). And in the specific example shown here, we could show that resistivity of this type of electrode improved by more than 20% when we increased the chuck temperature from 350°C to 800°C.

Figure 5 shows one excellent example for the bottom electrode deposition with the 8" VHC. What we see here is outstanding stress range (<110MPa), excellent sheet resistance (Rs) uniformity (< 0.8%) with very low specific resistivity (only 8.28 uOhm*cm) and impressive RC FWHM for such thin layer thickness (1.2°). This film performance exceeds all the bottom electrode specs developed with the original ESC chuck at 350°C.

The VHC deposition of Al_{1-x}Sc_xN is in the development phase at the moment, but it already shows promising results. In the example in Figure 6 we achieve the rocking curve FWHM below 1° with a chuck temperature of 600°C. Despite using mechanical wafer clamping for the very hot chuck tests here, we still see very similar stress and thickness profiles for the deposited film, suggesting that we can in principle preserve the stress and thickness uniformity developed with ESC chuck.

Last but not the least, the VHC also has the advantage of active chuck bias control with RF power applied to the chuck. The process tuning parameters remain the same as the original chuck type.

The way ahead

VHC looks set to provide a solution meeting the new challenges for further development of BAW technology. With heating capability to 800°C, we can improve the film crystallinity dramatically. In the meantime, we are also able to retain the film stress and thickness uniformity performance with the existing process kit and source. Film stress can still be controlled by RF bias on the chuck. This is a critical feature of the VHC as high temperature deposition on Si wafers usually leads to a very tensile thermal stress. The VHC has the capability to compensate the thermal stress with RF bias. Mechanical clamping is used for the current setup with backgas underneath the wafer for enhanced thermal coupling between the wafer and the chuck. To meet the demand for full-face deposition, we are developing a clampless version of VHC.

Overall, the flexibility and modular design of the CLUSTERLINE® platform places it in a strong position to cater to the changing needs of RF filter manufacturers and meet the challenges of future technology development. □

References

- M. Akiyama, K. Kano and A. Teshigahara, "Influence of growth temperature and scandium concentration on piezoelectric response of scandium aluminum nitride alloy thin films," *Applied Physics Letters*, vol. 95, p. 162107, 2009.
- K. Umeda, H. Kawai, A. Honda, M. Akiyama, T. Kato and T. Fukura, "Piezoelectric properties of ScAlN thin films for piezo-MEMS devices," *2013 IEEE 26th International Conference on Micro Electro Mechanical Systems (MEMS)*, pp. 733-736, 2013.
- S. Barth, H. Bartzsch, D. Gloess, P. Frach, T. Modes, O. Zywitzki, G. Suchanek and G. Gerlach, "Magnetron sputtering of piezoelectric AlN and AlScN thin films and their use in energy harvesting applications," *Microsystem Technologies*, vol. 22, pp. 1613-1617, 2016.
- R. Matloub, M. Hadad and P. Mural, "Piezoelectric coefficients of AlScN thin films in comparison," *2016 IEEE International Frequency Control Symposium (IFCS)*, pp. 1-2, 2016.
- S. Mertin, V. Pashchenko, F. Parsapour, C. Nyffeler, C. S. Sandu, B. Heinz, O. Rattunde, G. Christmann, M.-A. Dubois and P. Mural, "Enhanced piezoelectric properties of c-axis textured aluminum scandium nitride thin films with high scandium content: Influence of intrinsic stress and sputtering parameters," *2017 IEEE International Ultrasonics Symposium (IUS)*, pp. 1-4, 2017.
- Y. Lu, Dissertation: Development and characterization of piezoelectric AlScN-based alloys for electroacoustic applications, Albert-Ludwigs-Universität Freiburg im Breisgau, 2019.